Journal of Physics: Conference Series

PAPER • OPEN ACCESS

Beam extraction using non vacuum electron beam by reduced acceleration voltage

To cite this article: T Hassel *et al* 2018 *J. Phys.: Conf. Ser.* **1109** 012017

IOP Conf. Series: Journal of Physics: Conf. Series **1109** (2018) 012017 doi:10.1088/1742-6596/1109/1/012017

Beam extraction using non vacuum electron beam by reduced acceleration voltage

T Hassel[1], G Klimov[1] and A Beniyash[1]

[1] Institute of Materials Science, Leibniz University of Hannover, 30167 Germany

E-Mail: hassel@iw.uni-hannover.de

Abstract. One of the disadvantages of the non-vacuum electron beam (NVEB) systems is a high acceleration voltage, which leads to an increase of defence against X-ray radiation. Due to the reduced acceleration voltage. On the one hand, the size of the beam generator can be reduced, which leads to a significant weight reduction compared to the conventional EB technology, so that a robotic application comes in focus. On the other hand, the requirements for the X-ray protection are reduced because the penetration ability of the X-radiation decreases. For applications such as brazing, cladding and surface heat-treatment, by the low acceleration voltage non-vacuum electron beam (LAVNVEB) system is of great interest. Some of the first experiments on electron beam emission into the atmosphere with a low acceleration voltage (from 60kV and below) were carried out at an available LAVNVEB system at the Institute of Materials Science at the Leibniz University Hannover.

1. Introduction

Non Vacuum Electron beam technology (NVEB), to work with electron beams directly at the atmosphere is not a widespread technology in mechanical engineering. The main area of its application is mass production, such as automotive, where the main advantages of this type of welding are realized, namely: high productivity, independence from the surface properties of the material and possibility of integrating these plants into mass production lines. Most of the publications devoted to the NVEB dates from the 70th years of the last century. A new field of interest arose in the mid-90s due to the large-scale implementation of aluminum alloys into car bodies. The main disadvantage of non-vacuum welding is the scattering of the beam in the atmosphere and, as a consequence, the limitation of the working distance. In order to reduce beam scattering in NVEB systems, a high acceleration voltage of up to 175 kV is applied and all industrial non-vacuum systems are of this type. The disadvantages of high-voltage NVEB are large gun dimensions and intense X-ray radiation, which requires corresponding protection. A comparison of the necessary shielding for aluminum welding at 60 kV and 150 kV acceleration voltages is given in **Table 1** for the welding time of 100 h and 1000 h per year. The study of the possibility of beam emission into the atmosphere at relatively low accelerating voltages is of great scientific and industrial interest. In literature only few publications on this topic were found [1]. Recently, the Institute of Materials Science is working on the study of NVEB at low accelerating voltages. In the course of these works, an original electron-beam gun with a plasma cathode and a beam extraction system was developed for working under atmospheric conditions [2]. The following publication is devoted to the further development of these studies for the practical application of low-voltage non-vacuum electron beam system in the atmosphere.

Table 1: Overview of the necessary shielding for aluminum welding with max. 200 mA beam current for 60 kV and 150 kV acceleration voltage [3]

		100 h		**1000 h**	
		Acceleration voltage [kV]			
		60	150	60	150
Density [g/cm³]	**Material**	**Shielding thickness [mm]**			
11,3	Lead	1,25	4,5	1,5	5,4
7,9	Steel	8,2	63	9,8	75,6
1,8	Ceramic	250	460	300	525

2. Set-up for experiments

2.1. Available equipment

At the Institute for Material Science at Leibniz Universität Hannover are two NVEB systems. The one is NVEB welder PTR NV-EBW 25-175 TU with thermionic emission. The principle set-up of the NVEBW system is shown in **Figure 1.** This system has following specifications:

- Maximum beam power – 24.5 kW
- Maximum beam current – 140 mA
- Accelerating voltage – 175 kV.

Another is the NVEB welder with plasma EB emitters (self construction at IW). The principle set-up of the NVEBW system is shown in **Figure 1.** This system has following specifications:

- Maximum beam power – 4.2 kW
- Maximum beam current – 70 mA
- Accelerating voltage – 60 kV.

For the experiments on welding at low accelerating voltage, PTR NV-EBW 25-175 TU with thermionic emission was adapted and used.

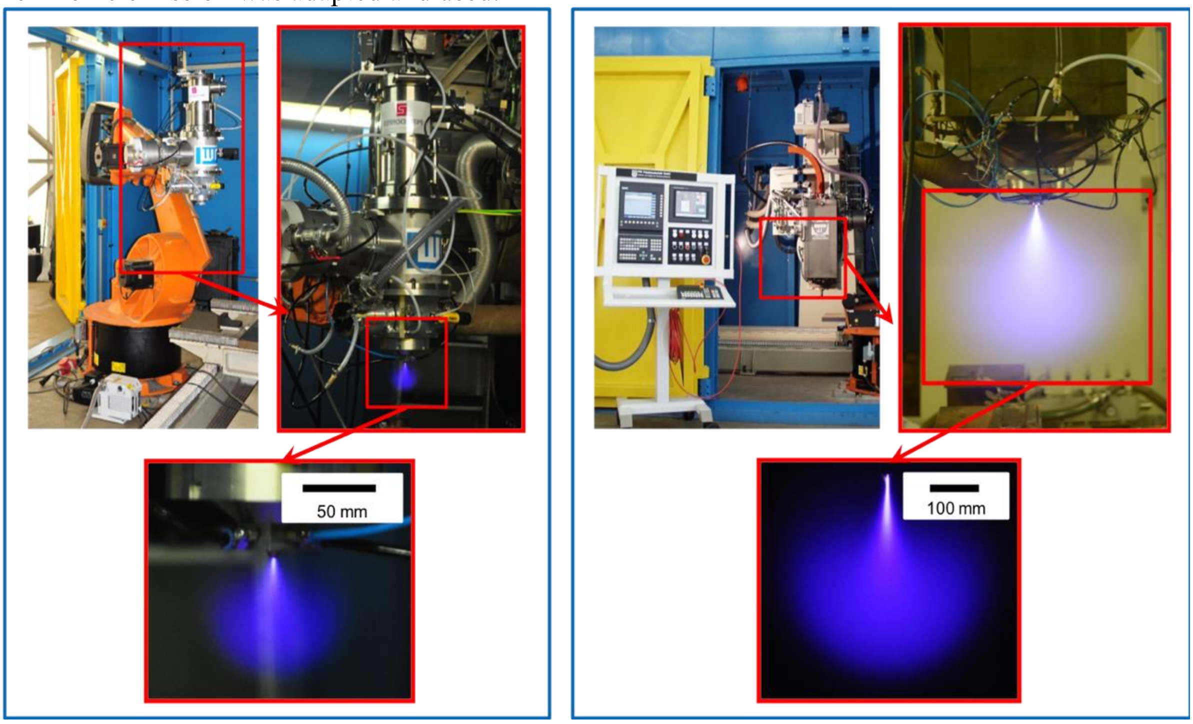

Figure 1. The principle set-up of the NVEBW system with thermionic emission (left) and plasma emitters (right)

2.2. Adaptation of equipment for tests

NVEB welder PTR NV-EBW 25-175 TU was constructed to work with an accelerating voltage of 175 kV. Before carrying out experiments on welding and brazing at low accelerating voltage, it must be adapted. The problem is that when the accelerating voltage decreases, the scattering of the electron beam in the vacuum system increases, what can lead to a collision of the equipment, for example inside nozzles and walls of vacuum stage system. For adaptation was changed accelerating gap. The acceleration gap was reduced by changing the length of the accelerating anode. For this purpose, the anode was increased to 8, 13 and 18mm. comparison of the influence of the length of the accelerating gap is presented in **Table 2**. During the experiment, the optimum values of the focusing and adjusting current were selected.

Table 2: Results of the efficiency and power measurements of the adopted NVEB system.

PTR-NVEB System Beam efficiency and power by 60 kV								
Beam current [mA]	**Efficiency [%]**				**Power [W]**			
	Original (0 mm) anode	**+8 mm anode**	**+13 mm anode**	**+18 mm anode**	**Original (0 mm) anode**	**+8 mm anode**	**+13 mm anode**	**+18 mm anode**
20	71,1	**75,8**	64,3	33,8	853	**910**	772	406
25	70,5	**76,9**	64,8	34,2	1058	**1154**	972	513
30	69	**80**	63,7	34,7	1242	**1440**	1147	625
35	67	**78,1**	66,8	37,4	1407	**1640**	1403	785

Measurements show that shortening of the acceleration gap by 8 mm gives the most optimal efficiency and power. Further experiments on welding and brazing were carried out on an adaptive NVEB system.

2.3. Low acceleration study

At first we made a study to investigate the possibility to produce an effective electron beam usable as a tool for welding at different acceleration voltages on the PTR welder.

We mentioned that it is possible by the variation of the acceleration gap to copple out the e-beam on the atmosphere up to an acceleration voltage of 30kV, see **Figure 2**.

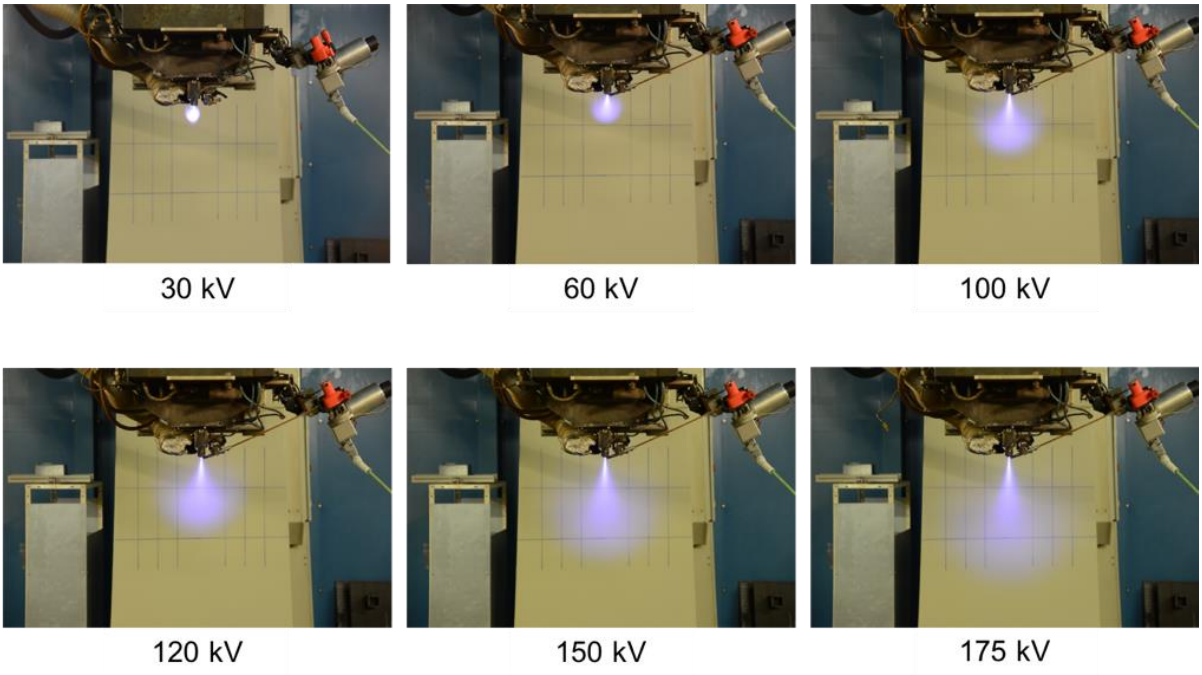

Figure 2: The electron beam plume at the atmosphere by different value of acceleration voltage and 30 mA of beam current.

2.4. Selection of materials
The following materials were used for welding experiments:
- 22MnB5 with 1mm thickness
- DP500 with 1,5mm thickness
- CU-ETP with 1.5mm thickness

The following materials were used for brazing tests:
- Composite solder wire: AlCuSi with diameter 1.2 mm
- Standard solder wire: AlSi12 with diameter 1.6 mm
- Base material: AW6063

3. Welding and brazing tests with 60kV acceleration voltage and their results

3.1. Welding tests and results
To prove the possibility of using NVEB by 60kV acceleration voltage, welding experiments were carried out. After determining the optimal parameters were carried out a metallographic analysis of the welds, **Figure 3.**

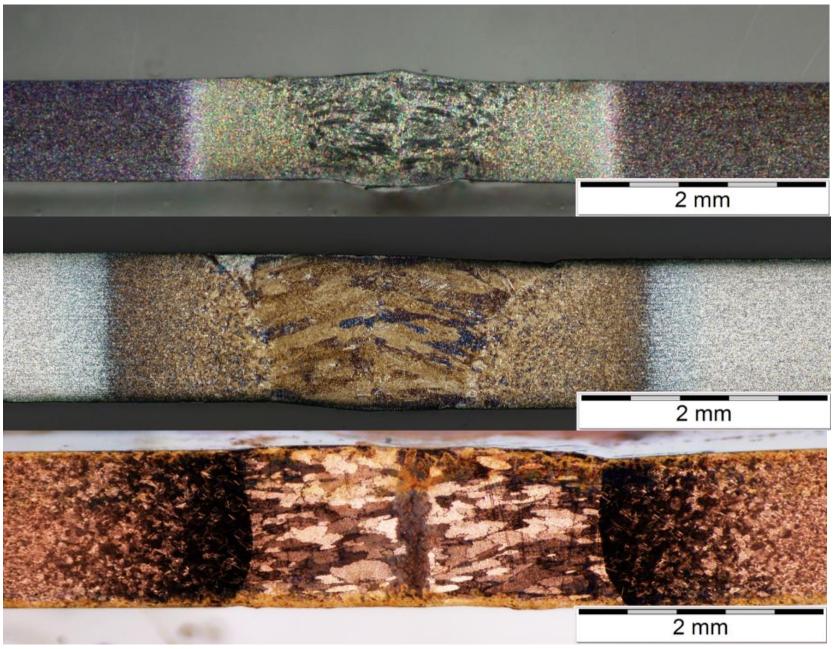

Steel 22MnB5 1mm:
I_S=25 mA,
v_W=1.8 m/min,
a= 8 mm

Steel DP500 1.5 mm
I_S=60 mA,
v_W=2 m/min,
a= 10 mm

Cupper CU-ETP 1.5 mm
I_S=130 mA,
v_W=2 m/min,
a= 10 mm

Figure 3: Macrosections of the weld samples (I_S- beam current, v_S- welding velocity and a- work distance)

Metallographic analysis of welded joints shows the absence of defects in the weld seam. In addition, a suitable formation of the root of the seam is observed. From these results, the NVEB technology with 60kV acceleration voltage can be used for welding of thin sheets from steel and copper.

3.2. Brazing test and results
Before running of experiment aluminium brazing experiments, the surface of the base material must be etched to remove the oxide layer in order to improve the quality of the connection between the solder and the base material. **Figure 4** shows the macrophotographs of the compounds obtained.

IOP Conf. Series: Journal of Physics: Conf. Series **1109** (2018) 012017 doi:10.1088/1742-6596/1109/1/012017

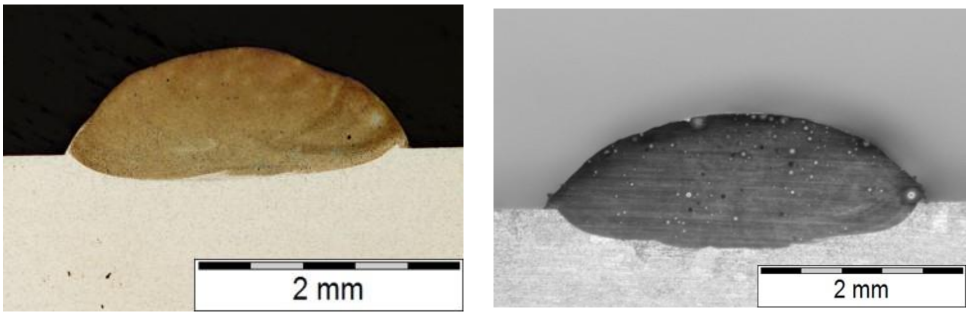

AlSi12 Ø1,6 mm
60 kV, 28 mA,
v_L:1,5 m/min, v_D:1,5 m/min
Wetting angle: 60,4°
Depth of fusion: 209 µm

AlCuSi, Ø1,2 mm
60 kV, 35 mA,
v_L:1 m/min, v_D:2 m/min
Wetting angle: 52°
Depth of fusion: 489 µm

Figure 4: Macrosections of AlCuSi and AlSi12

Metallographic analysis shows a good contact angle with the surface using brazing by NVEB at 60kV acceleration voltage. The analysis of macro sections shows a slight pore formation for samples from AlSi12 wire and more intense pore formation for the sample from AlCuSi. This defect in aluminum alloys is most often associated with the presence of hydrogen in the melt. The source of hydrogen can serve as an atmosphere during the process, insufficiently smoothed surface of the base material and filler wire [4].

Metallographic analysis of the joints shows the suitability for the brazing process the NVEB by 60kV acceleration voltage.

4. Development of the vacuum stage system for Plasma cathode

To extract the beam into the atmosphere, it is necessary to have a vacuum stage system. One of the important details of this vacuum system is a crossjet. Crossjet serves to divert the intake gas flow through the orifice by using a transverse flow of gas. The composition of the intake gas includes air, smoke and metal steam during the process, all together have a very negative effect on the vacuum system and, consequently, on the characteristics of the electron beam. The scheme of the vacuum stage system is shown in **Figure 5**.

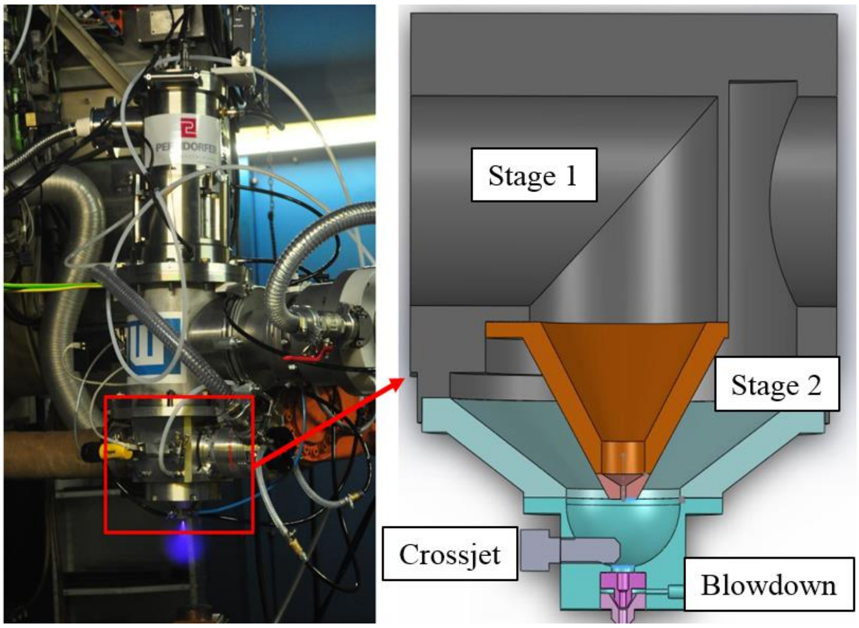

Figure 5: Vacuum stage system of the NVEB with a plasma gun

As an alternative to crossjet, a deflector can be used. Due to its geometry, the deflector can deviate the suction gas flow without using a transverse gas flow, see **Figure 9**.

4.1. Selection of deflector geometry

Selected types of deflector geometry are shown in **Figure 6**. **Figure 6a** shows the currently used crossjet, but without a hole for the deflecting flow. The images **Figures 6b-6d** depict the types of geometry under study.

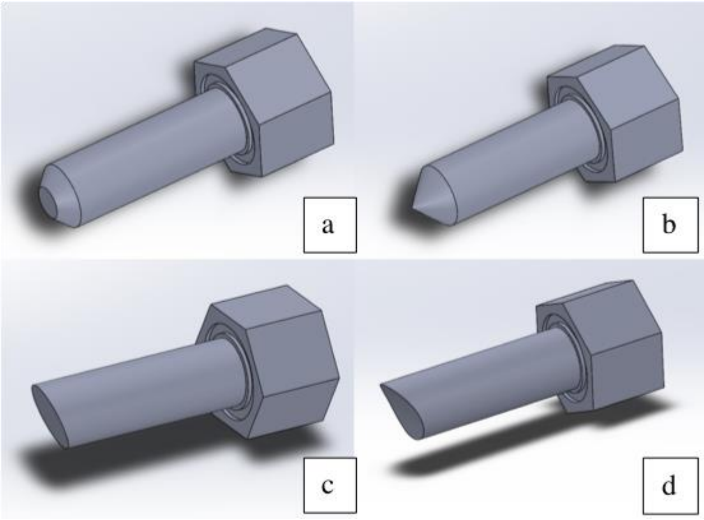

Figure 6: The CAD geometries of deflector.

4.2. FEM analysis using ANSYS® CFX®

The system designed for this application was subsequently evaluated using ANSYS® CFX® [5]. Of special interest was the gas-dynamic effect of deflectors. The deflector is located exactly at the point where the air expands after exiting through the orifice.

For the simulation, the medium was set as air with ideal gas properties. The surrounding atmosphere was introduced as an opening with standard conditions for temperature (293 K) and pressure (1013 mbar). Only the first and second stage were part of the simulation, as the high-vacuum conditions present in the beam emitter chamber are not covered by the mathematic description used in ANSYS® CFX® [2]. See **Figure 7** and **Figure 8** for pressure contour plots and chart along the beam axis gathered from this simulation. The pumps were introduced as normal velocity at the outlets. The speed was set to represent to pumping speed that can be expected from the pumps used for the system and the length of the tubing. The **Figure 8** shows the pressure chart along the beam axis for the crossjet and different geometries of defelctor. In the **Table 3** are shown the average values of pressure along the beam axis for the stage 1.

IOP Conf. Series: Journal of Physics: Conf. Series **1109** (2018) 012017 doi:10.1088/1742-6596/1109/1/012017

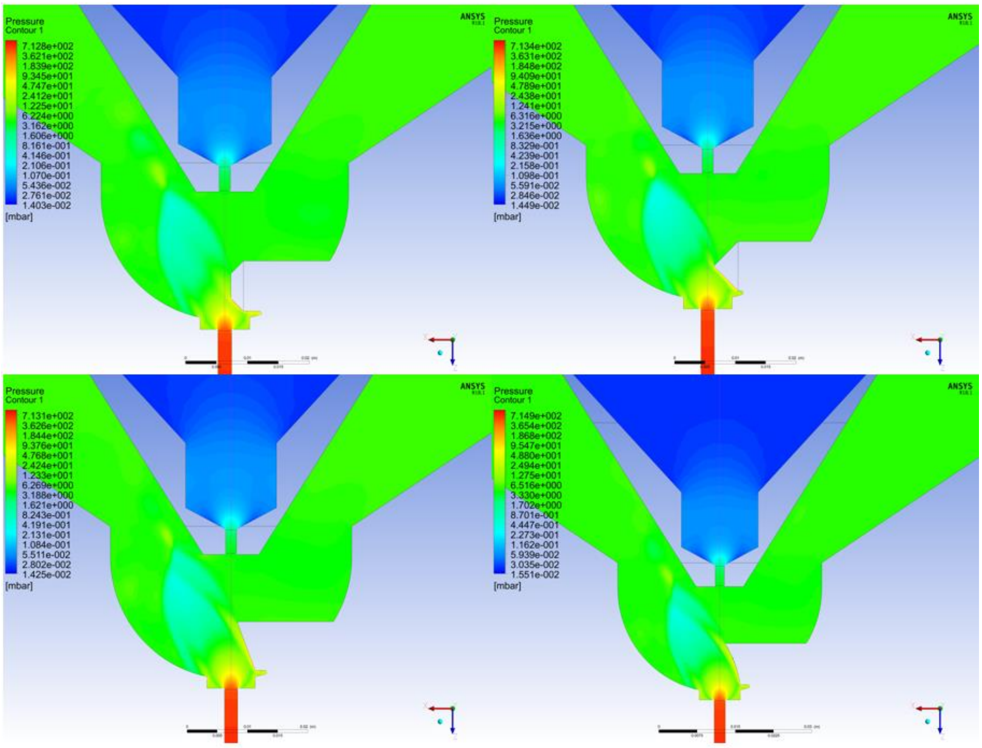

Figure 7: Pressure distribution at the different geometries: crossjet (left top), deflector 1 (right top), deflector 2 (left down) and deflector 3 (right down)

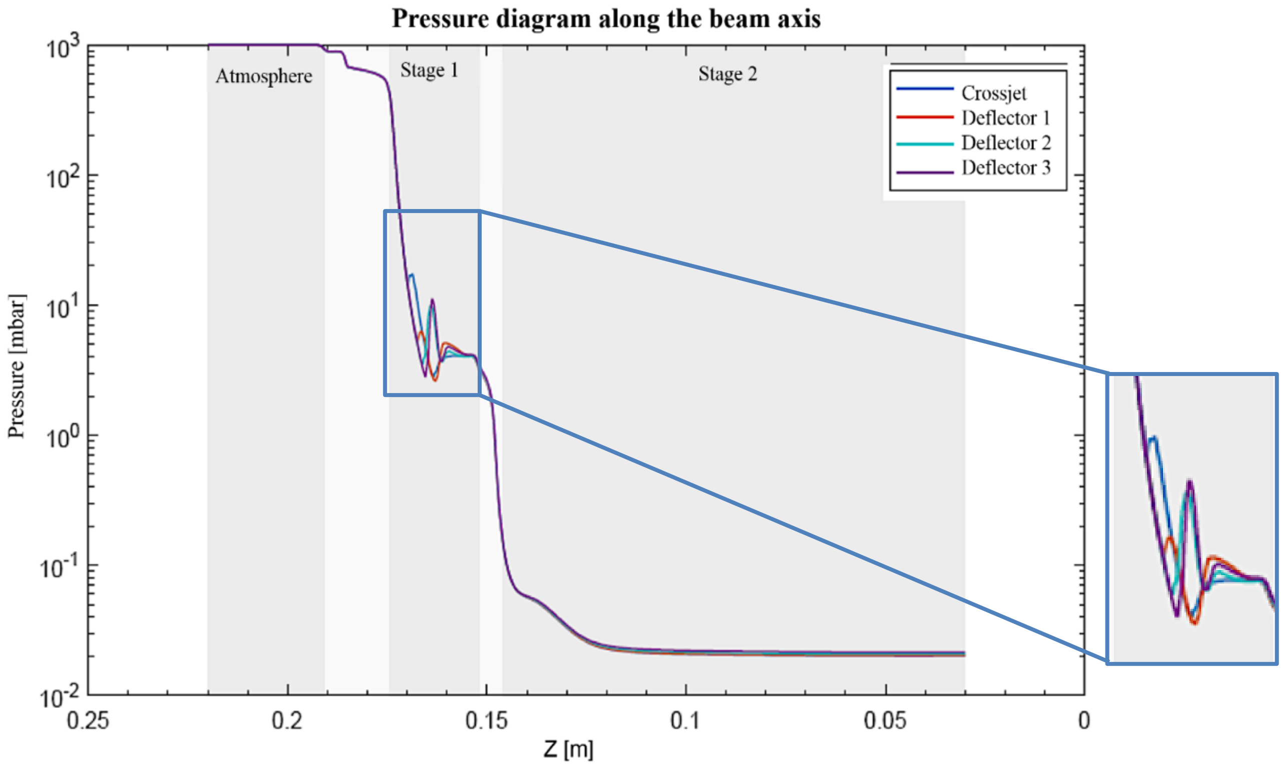

Figure 8: Simulated pressure diagram along the beam axis for the crossjet and different designs of the deflectors

Figure 8 shows, that the crossjet and deflectors have the big influence on the pressure in the stage 1. Further in this work the behavior in the 1 stage will be observed und discussed

Table 3: Average pressure values along the beam axis at the stage 1

	Crossjet	Deflector 1	Deflector 2	Deflector 3
Pressure [mbar]	6,43	5,53	5,92	5,91

The FEM Analysis shows that the use of deflector 1 gives better conditions for vacuum along the beam axis compared to other types of geometry and crossjet. But the use of such a geometry can lead to a greater turbulence in the first stage than the 2 and 3 geometry of deflector. Analysis of the distribution of pressure in the 1 stage, showed that using the deflector 2, leads to an optimal value of the pressure in the system in comparison with the other investigated geometries. The distribution of the pressure in the first stage is shown in the **Table 4.**

Table 4: Average pressure at the stage 1 for the crossjet and different geometries of the deflectors.

	Crossjet	Deflector 1	Deflector 2	Deflector 3
Pressure [mbar]	6,53	6,46	5,76	6,56

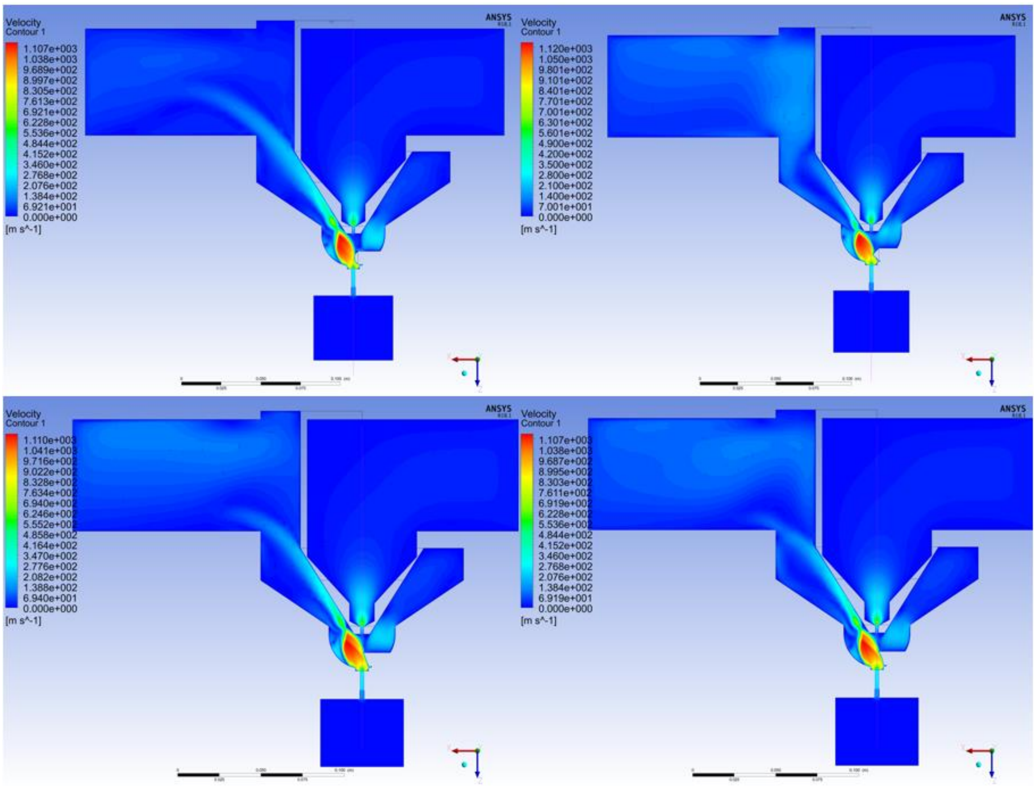

Figure 9: Velocity distribution at the different geometries: crossjet (left top), deflector 1 (right top), deflector 2 (left down) and deflector 3 (right down)

Figure 9 shows that using the crossjet, velocity among the beam is lower than velocity obtained from deflectors. The deflector 1 leads to the most turbulence in stage 1. The 2 and 3 deflectors produce almost the same turbulence in stage 1 and their application raises the flow velocity along the beam axis.

4.3. Manufacturing and testing of the deflectors

The different deflectors were subsequently built and tested. The pressure was measured at the stage 1. To verify the ANSYS simulation the measured pressures in the system are compared to results from the simulation. The simulated and measured results are shown at the **Table 5**.

Table 5: The comparison of simulated and measured pressure at the stage 1 for the crossjet and different deflectors.

Stage 1 pressure [mbar]	**Simulation**	**Measurment**
Deflector 1	6,46	3,00
Deflector 2	5,76	3,00
Deflector 3	6,56	3,00
Crossjet	6,53	5,90

From **Table 5** it can be seen that the use of a deflector in place of a crossjet leads to an improvement in the vacuum in the system. All 3 types of deflector have the same effect on the pressure in the first stage. Application of deflectors leads to reduction of the pressure to compare with the crossjet.

5. Conclusions and outlook

In this paper, it was proved the suitability of using NVEB by 60kV acceleration voltage for the processes of welding (steel and copper) and of brazing of aluminum. In the future it is planned to investigate the possibility of welding and additive manufacturing of metals. In addition, it is necessary to compare the results of welding using a plasma gun.

FEM analysis has shown that a standard crossjet can be replaced by a deflector to divert the intake gas flow through the orifice and leads to an improvement in the vacuum in the vacuum step system.

6. Aknowledgments

Parts of the results were obtained from the research project No. 06.114 of the DVS, which was funded by the Federal Ministry of Economics and Energy through the AIF.

References

[1] Arata, Y.; Tomie, M. Some Fundamental Properties of Nonvacuum Electron Beam. *Transactions of the Japan Welding Society*, *1970*, 40–59.
[2] *Beam technologies & laser application*. *Proceedings of the international scientific and technical conference, 21-24, September, 2015, Saint-Petersburg, Russia;* Turichin, G.A., Ed.; Publishing House SPbSPU: Saint-Petersburg, 2016.
[3] Berger, M.J.; Inokuti, M.; Anderson, H.H.; Bichsel, H.; Dennis, J.A.; Powers, D.; Seltzer, S.M.; Turner, J.E. Report 37. *Journal of the International Commission on Radiation Units and Measurements* **1984**, *os19*, NP-NP, doi:10.1093/jicru/os19.2.Report37.
[4] Ostermann F., 2005,"Schweißen von Aluminiumwerkstoffen," pp. 435–468.
[5] ANSYS® Academic Research, Release 18.1